


Catastrophic Interference is Mitigated in Naturalistic Power-Law Learning Environments

Atith Gandhi*, Raj Sanjay Shah*, Vijay Marupudi, Sashank Varma

Georgia Institute of Technology 

{ agandhi98, rajsanjayshah, vijaymarupudi, varma }@gatech.edu

Abstract

Neural networks often suffer from catastrophic interference (CI): performance on previously learned tasks drops off significantly when learning a new task. This contrasts strongly with humans, who can sequentially learn new tasks without appreciably forgetting previous tasks. Prior work has explored various techniques for mitigating CI such as regularization, rehearsal, generative replay, and distillation methods. The current work takes a different approach, one guided by cognitive science research showing that in naturalistic environments, the probability of encountering a task decreases as a power-law of the time since it was last performed. We argue that realistic evaluation of techniques for the mitigation of CI should be performed in *simulated naturalistic learning environments*. Thus, we evaluate the extent of mitigation of CI when training simple rehearsal-based methods in *power-law environments* similar to the ones humans face. Our work explores this novel rehearsal-based approach for a domain-incremental learning task: learning permutations in the MNIST task. We first compare our rehearsal environment with other baselines to show its efficacy in promoting continual learning. Additionally, we investigate whether this environment shows *forward facilitation*, i.e., faster learning of later tasks. Next, we explore the robustness of our learning environment to the number of tasks, model size, and amount of data rehearsed after each task. Notably, our results show that the performance is comparable or superior to that of models trained using popular regularization methods and also to rehearsals in non-power-law environments. The benefits of this training paradigm include simplicity, learning that is agnostic to both tasks and models and the lack of a need for extra neural circuitry. In addition, because our method is orthogonal to other methods, future research can explore combining training in power-law environments with other continual learning mechanisms.

Introduction

Humans learn to perform new skills throughout their lifetime without appreciable forgetting of old skills. Within the context of machine learning (ML) algorithms, the ability to incrementally acquire new knowledge while retaining previously learned experiences is known as *continual learning* or *lifelong learning* (Mitchell et al. 2018; Parisi et al. 2019). ML models are typically trained to perform a single task.

*These authors contributed equally.
Copyright © 2024. All rights reserved.

They would be much more useful in the real world if they could sequentially learn new tasks and remember multiple old tasks over time. However, when models try to learn new tasks, this often leads to a drastic drop in the performance of old (i.e., previously learned) tasks. This phenomenon is known as *catastrophic interference* (CI), and it is a major challenge for ML models. The current study looks to cognitive science to simulate the distribution of data observed in human-like learning environments and explores the mitigation of CI in deep neural networks trained in such naturalistic environments.

Neural network models are capable of learning to perform a variety of tasks. However, because of CI, when a new task is introduced, these models must be trained on the new task as well as all old tasks. Unfortunately, this is computationally inefficient. Ideally, neural networks should learn continuously, incrementally acquiring new tasks while minimally forgetting prior tasks. A secondary desideratum is that the effort to learn a new task should not explode as the number of previously learned tasks increases. That is, an ideal learning model should show *forward facilitation*, or faster learning of new tasks based on knowledge of previously learned tasks.

There is extensive research on methods to mitigate CI in ML models and also promote forward facilitation. These include weight regularization, selective forgetting, and memory replay to strengthen the performance of previously learned tasks (Wang et al. 2023). These research methods are tested on the static availability of samples of each task, which is not representative of how tasks repeat in natural environments. Here, we introduce a different approach, one that derives from cognitive science studies of naturalistic learning environments.

Naturalistic cognitive learning environments

Anderson and Schooler (1991), following a Bayesian analysis of naturalistic environments, found that the probability of needing to retrieve a particular item from memory declines as a power function of the time since that item was last retrieved. Their data came from a range of linguistic environments where words re-occur: newspaper headlines, the utterances of parents around children learning to speak, and email messages. Their findings have been replicated (Schooler and Anderson 1997) and extended to environments ranging from laboratory studies of human memory (Anderson et al. 1997)

Various data where power-law frequency distribution is observed	References
Re-tweets	(Cvetojevic and Hochmair 2018; Lu et al. 2014)
The frequency of occurrence of unique words in a novel (Zipf’s Law)	(Newman 2005)
Number of distinct interaction partners in protein interaction networks	(Ito et al. 2000)
Degree of known nodes in the internet network representation in autonomous systems	(Holme, Karlin, and Forrest 2007)
Number of long-distance calls received in the United States in a single day	(Abello, Buchsbaum, and Westbrook 2002; Aiello, Chung, and Lu 2000)
Number of unique signers required for sign language recognition algorithms to recognize signs accurately	(Bhardwaj et al. 2024)
Number of examples of a particular sign required for sign language recognition algorithm to accurately recognize a particular sign	(Bhardwaj et al. 2024)
Test errors in deep learning algorithms follow a power-law with the number of samples seen per example	(Meir et al. 2020)
Number of people affected by electrical blackouts in the United States between 1984 and 2002	(Newman 2005)
Average price of NFTs by categories	(Nadini et al. 2021)
Degree of items in recommender system graphs	(Milojević 2010; Newman 2005)
Prompts in text to image models (Diffusion DB)	(Xie et al. 2023)
Phoneme frequencies in collection of illustrative texts	(Baird, Evans, and Greenhill 2022)

Table 1: Empirical evidence for power-law frequency distributions occurring naturally

to field studies of the social environment of chimpanzees (Stevens et al. 2016).

Real-world environments follow power-law distributions. Table 1 shows a non-exhaustive list of data where such frequency distributions are observed. Moreover, human learning appears to be tuned to these statistics, with the practice of skills improving their performance (i.e., speed, accuracy) according to a power law (Newell and Rosenbloom 2013). **Given the large number of real-world contexts where data repeats according to a power-law frequency distribution, we argue that rehearsal-based techniques for mitigating CI should be tested on simulated naturalistic learning environments where rehearsal follows the same frequency distribution.** This supports the strategy of not storing examples of previous tasks by design but only rehearsing those examples that recur naturally. For example, in the context of modern language modeling algorithms, this is akin to learning a semantic distribution shift by incrementally pre-training over real-time streaming data (such as social media feeds on Twitter).

Taking inspiration from this characterization of natural environments (Anderson and Schooler 1991), Lyndgaard et al. (2022) investigated whether training in power-law environments mitigates CI. They trained a neural network on a sequence of tasks, with the proportion of training samples for a previous task decreasing as a power function of the number of intervening tasks. As predicted, there was virtually no CI. This study, although suggestive, contained several limitations: the training tasks were extremely simple (i.e., sequentially learning the boolean functions AND, OR, XOR, and NAND), they did not include an upper baseline, they did not compare performance to training in alternate non-power-law environments, and they did not evaluate whether this approach scales to a greater number of tasks. Here, we perform a significantly more comprehensive evaluation of the mitigation they observed in such power-law environments.

Research Questions:

The current study simulates a naturalistic power-law learning environment and evaluates its efficacy for mitigating CI. It uses tasks that are standard in the continual learning literature

(i.e., permuted MNIST), compares performance to appropriate upper and lower baselines, compares performance to a representative CI mitigation approach (EWC), and compares performance to training in other, non-power-law training environments. In more detail, the study addresses the following research questions:

1. **Simulation:** Can we simulate rehearsal methodologies (i.e., power-law training environments) inspired by the naturalistic learning environments of humans?
2. **CI Mitigation:** What is the extent of CI mitigation when using natural rehearsal in power-law training environments?
 - (a) How does this training environment compare to current baselines?
 - (b) Does the mitigation persist across variations in model architecture?
 - (c) How many tasks can the model learn in a power-law training environment without exploding in the computation required to learn a new task, while also maintaining high accuracy on previously learned tasks?
3. **Forward facilitation:** To what extent does the power-law training environment promote forward facilitation?
4. **Optimized rehearsal:** In a power-law environment, what fraction of old training data needs to be maintained to still observe mitigation of CI?
5. **Restricted training environments:** Real-life situations do not have an unlimited budget for memory to store samples for future rehearsal. How can we account for memory-based constraints?
 - (a) Can we modify the power-law training environment setup to account for realistic limitations on memory?
 - (b) Can we stress test the mitigation properties of the power-law environment under restrictions of increasing severity?
 - (c) In the restricted context, how does training in the power-law environment compare to training in other rehearsal-based environments?
6. **Evaluation:** Can we devise new metrics for the evaluation of mitigation of CI?

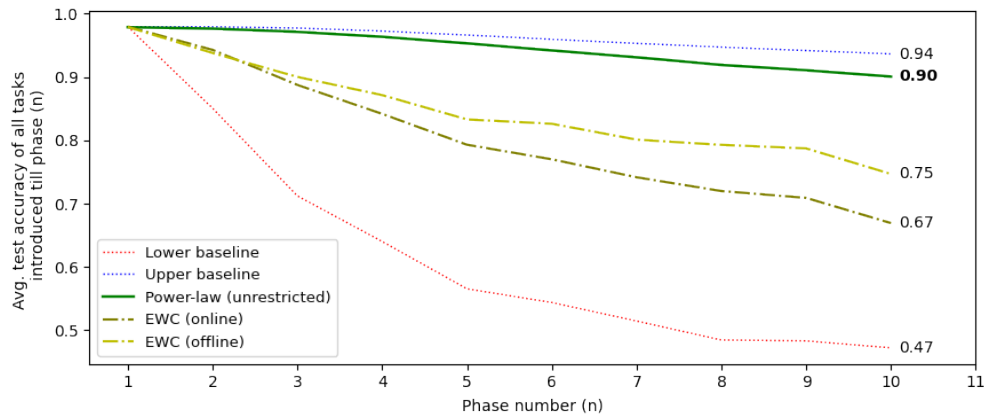


Figure 1: Comparison of all the baselines and training environments on the Permuted MNIST task with 10 phases. The power-law training environment performs most similarly to the upper baseline at the end of phase 10.

Related Work

There is a considerable body of research in continual learning or lifelong learning in neural networks (McCloskey and Cohen 1989; Mitchell et al. 2018; Parisi et al. 2019; Thrun and O’Sullivan 1996). Methods to mitigate CI largely fall into four major categories: distillation-based, parameter-isolation, regularisation-based, and rehearsal-based methods.

Distillation-based methods (also known as pseudo-rehearsal methods) assume that samples from previously learned tasks are minimally available. Therefore, these methods use the trained network outputs from the previous rounds as approximations for the previous task samples (Robins 1995). For example, Learning without forgetting (Li and Hoiem 2017), or LWF, performs knowledge distillation by keeping track of model outputs for the same input samples over different phases and computes a combined loss over the ground truth new task output with old model output stored in memory. This technique can potentially lead to error propagation and gradual erroneous behavior build-up over learning phases. More generally, *the success of these methods depends on model performance on previous tasks and the difficulty of the new task being introduced.*

Parameter-isolation approaches (Mallya and Lazebnik 2018; Serra et al. 2018) seek to isolate those neural network weights that have a greater probability of being relevant to previous tasks. Mallya and Lazebnik attempt to iteratively prune redundant parameters in a neural network to free up capacity to learn new tasks. Taking a different approach, Hard Attention Networks (Serra et al. 2018) mask different areas of neural network layers to explicitly allocate network capacity to different tasks. Note that *these approaches are model architecture-dependent and may not generalize to all training algorithms.*

Many recent works explore weight regularization techniques (Kirkpatrick et al. 2017; Zenke, Poole, and Ganguli 2017; Li and Hoiem 2017; Rusu et al. 2022). One popular technique, elastic weight consolidation (EWC) (Kirkpatrick et al. 2017), slows down adjustments to existing weights based on their importance to previously learned tasks. EWC’s

regularization term was later improved to handle a greater number of tasks without increasing computation cost; this new approach was termed online EWC (Schwarz et al. 2018). Similarly, Zenke, Poole, and Ganguli propose the use of *intelligent synapses* that mimic the complexity of biological synapses. During training, the importance of each synapse is computed by considering its local contribution to the change in the global loss. This helps prevent the loss of information from changing synapses important for a particular old task while learning a new task. Many other regularization techniques attempt to determine the importance of weights during regularization (Lee et al. 2017) and increase the penalty for altering the important weights. However, recent literature (van de Ven, Tuytelaars, and Tolias 2022) shows *that regularisation methods fail to scale up with the complexity of tasks while rehearsal-based methods show better mitigation of CI.*

Rehearsal-based methods

The fourth category is composed of rehearsal-based methods, also known as replay-based methods (Hayes and Kanan 2019; Lopez-Paz and Ranzato 2017; Xu et al. 2009). These methods use some learning samples from previous tasks as training samples upon the introduction of a new task. The samples of previous tasks can either be retained in a buffer upon introduction (iCARL, ER) or generated by a separate generative model (DGR, BI-R). One popular rehearsal method, Experienced Replay (ER) (Rolnick et al. 2018), stores a fixed number of samples from the old tasks while learning the new task. Another is incremental Classifier and Representation Learning (iCaRL) (Rebuffi, Kolesnikov, and Lampert 2016), which combines the LwF algorithm with some exemplars stored from the previously seen tasks. One generative rehearsal-based method is Deep Generative Replay (Shin et al. 2017a), where a copy of the generative model and classifier is stored and used to generate and labels data from previous tasks and add them to the training data. This generative process is modified in Brain-Inspired Replay (van de Ven, Siegelmann, and Tolias 2020) to handle more and complex tasks by taking inspiration from complementary memory

Property	Value
Number of fully connected hidden layers	1 - 5
Number of units per layer	1000
Dropout probability	0.5
Learning rate	0.003
Batch size	2048
Maximum training iterations per task	100
Optimizer	Adam
Loss function	Categorical cross-entropy
Early stopping	No

Table 2: Details of the model architecture.

systems of the mammalian brain. Most rehearsal-based methods calculate complex measures to find exemplars to anchor certain weights to previous tasks and perform guided distribution shifts. These measures are often dependent on training parameter choices and loss calculations, making them harder to scale to new problem spaces. By contrast, the power-law training environment-based rehearsal approach we propose is model-agnostic and task-agnostic and can be easily set up for any task.

CI mitigation techniques inspired from cognitive science literature

Our method for mitigation of CI is inspired by cognitive science research on how frequently humans experience previously seen tasks (Anderson and Schooler 1991) and the initial computational explorations by Lyndgaard et al. (2022). ML researchers have previously explored mitigation techniques inspired by human behavior. Davidson and Mozer investigated how a standard convolutional neural network performs classification tasks when new visual tasks are introduced sequentially, simulating the way humans learn as they become experts in a particular domain. Another method, REplay using Memory INdexing (REMIND) (Hayes et al. 2019), is inspired by how the brain indexes memories, and explores efficient replay strategies with compressed vector representations. Fearnert (Kemker and Kanan 2017), inspired by the complementary learning systems of the mammalian brain, uses different networks for long-term and short-term memory in pseudo-rehearsal. We note that no prior studies have explored the impact of naturalistic environmental structure on learning. The current study simulates this structure to build a novel rehearsal methodology to mitigate CI.

Methodology

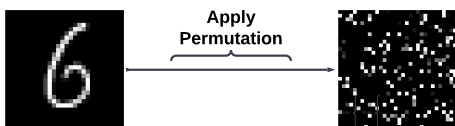


Figure 2: Permutation transformation on a sample image.

Our work follows others (Goodfellow et al. 2015; Kirkpatrick et al. 2016) in evaluating the power-law training environment on the permuted MNIST task. The dataset for the task and the details of the training environment are described below.

Domain Incremental Learning scenario

In this learning scenario, the problem structure has a shift in the input distribution but has the same possible output space as the previous tasks (van de Ven, Tuytelaars, and Tolias 2022). Examples of Domain Incremental Learning scenarios (Domain-IL) are object detection tasks or classification tasks with a change in contexts; like detecting polar bears in images with the background of mountains vs. floating ice bodies or finding sarcasm on different platforms such as Reddit and Twitter. While Domain-IL tasks are not as difficult as Class incremental tasks for ML models, they remain the most popular forms of continual learning problems in practice (van de Ven, Tuytelaars, and Tolias 2022; Dai et al. 2023). We focus on the Domain-IL scenario because of this real-world demand.

Dataset

The MNIST dataset (Deng 2012) contains 60,000 training images and 10,000 test images, each 28x28 pixel grayscale image of a single handwritten digit. For building the permuted MNIST task, we add padding to the images to rescale them to 32x32 pixel images and then generate a fixed, random permutation by which the input pixels of all images are shuffled as shown in Figure 2. The model learns to identify the number corresponding to the digit despite the permutation. Each task is associated with a characteristic permutation, and the same permutation is applied across the entire dataset. The tasks formed by the transformations follow the domain-incremental learning task described by (van de Ven and Tolias 2019; Kirkpatrick et al. 2016), where the task identity is not available during performance.

Model architecture

Our model consists of fully connected multi-layer perceptrons with the properties shown in Table 2. The network architecture is inspired by the experiments from prior studies (van de Ven, Tuytelaars, and Tolias 2022). Most of the experiments in the current study are performed with three layers; note that we also show the model size-agnostic nature of our training environment by varying the number of layers. For a fair comparison between the learning environments discussed in the section *Training Environment Setup*, the same model architecture is used in all environments. Finally, in all of our experiments, we use 5 seeds to show reproducibility and robustness to the initialization of weights in a network.

All experiments were conducted with PyTorch (Paszke et al. 2019) on NVIDIA RTX 2080 GPUs with 12GB GPU RAM.

Training environment setup

We introduce a new task in each **phase** or episode of training, for a total of 10 phases. In each phase, the new task is introduced with the maximum number of samples (60,000) along with some data from the previously learned tasks (rehearsal data). The training environment describes the size, and the task distribution of the data to be rehearsed. All of the training environments considered here are described below. Refer to the Appendix for the data distribution for each one.

Baselines: This work uses three techniques as baselines to show the efficacy of a power-law training environment.

- **Lower-baseline:** We establish a *lower-bound performance baseline* for our tasks. In this training setup, each training phase will only have access to the data for the newly introduced task, and there will be *no rehearsal of the previous tasks*. This is akin to a regular neural network architecture which sequentially learns new tasks. This environment is expected to show high levels of CI.
- **Elastic Weight Consolidation (EWC and EWC (online)):** EWC (Kirkpatrick et al. 2016) is a regularization-based approach where the model adapts the weight-updating process to limit the shift in weights that are relevant to previous tasks. This method is the baseline approach for regularization-based methods. EWC (online) uses a different regularization term to make it computationally scalable for a larger number of tasks.
- **Upper-baseline:** In this baseline case, each training phase will have access to the data samples of the introduced task along with *all of the samples of the previous tasks*. This case serves as the upper-bound performance baseline. Thus, in the last phase, the model will train over the entire data from all the tasks. This environment is expected to show the least amount of CI, though at the expense of maximum resource usage (and, as we will see, reduced forward facilitation).

Unrestricted memory

In this environment, we compare our proposed power-law setup to the baseline distributions without any restrictions on the maximum number of rehearsal samples in a phase.

Proposed power-law distribution: Each training phase of this setup has the maximum number of samples for the introduced task, while the data distribution for the previous tasks follows a decreasing power function such that the task introduced in the first phase (the oldest task) will have the least representation. This corresponds to naturalistic human learning where humans see rehearsals of tasks at a decreasing power function frequency. The power-law sample distribution equation is given by equation (1), where the values for x range from one to the maximum number of phases (10).

$$f(x) = ax^{-b} \quad (1)$$

RQ 4 explores optimization or the impact of different power-law distribution curves in mitigating CI, by varying the minimum number of samples for task 1 in the last phase. Anchoring the following sample sizes in different phases for each task – the maximum number of samples when introducing a new task and the minimum number of samples of task 1 in the last phase – allows us to compute the constants a and b in eq 1. The obtained values for these constants for the different power-law curves in our experiments are given in the Appendix Table 9. The matrix formed with the sample distribution of each task in each phase is persymmetric in nature; see Appendix Table 12.

Restricted Training Environment

Real-life model training situations do not have an unlimited budget for memory. Restrictions on memory mean that models can only see a limited number of samples at training time. An important goal is to investigate different memory budgeting strategies for training new tasks while performing rehearsal of old tasks. This study looks at the impact of memory constraints on the mitigation properties of the power-law environment under different budgeting strategies (RQ 5).

We simulate such restricted rehearsal by allocating a memory budget as a percentage of the sample size of the new task. We test rehearsal percentages of 0.1%, 5%, 10%, 25%, 50%, 75%, and 100%. After allocating the total memory budget in each phase, we evaluate different sampling strategies by distributing task rehearsal across phases in three different ways: power-law, exponential, and uniform, all with the same budget. Since the restriction is set to the total number of examples from previous tasks and the sum of samples of rehearsed tasks is fixed, we fit the distributions and rescale to satisfy the summation constraint. It is important to note that distribution types are across samples for each task over phases as opposed to rehearsal task distributions in each phase. This leads to different power-law / exponential curves for each task. We do this to best simulate a human-like training environment, where samples from previous tasks decline over phases in a power-law-like (or potentially exponential-like) manner. This is one way of operationalizing restricted rehearsal which mitigates CI for the permuted MNIST tasks. Problems of different complexities may require different power-law restricted rehearsal operationalization based on the task. The details of the operationalization for the modified power-law distribution, the modified exponential distribution, and the uniform distribution are given in the Appendix.

Results

First, we compare the performance of the power-law training environment with the baseline approaches and with EWC in the unrestricted memory scenario discussed above. Figure 1 and Table 4 shows the average test accuracy over all tasks after 10 phases. Table 4 also shows the average test accuracy over 20 phases to test whether increasing the number of phases/tasks leads to a drop in mitigation performance for all training environments. We note the following key takeaways:

- All approaches perform better than the lower baseline, showing that including examples of previously learned tasks or using regularization-based methods mitigates CI.
- Rehearsal methods; methods that have access to previous task data, perform better than the methods where no such data are included.
- Power-law performs considerably better than all other training environments except the upper baseline. Notably, it uses half the number of total samples as the upper baseline across the ten phases (1.5 vs 3.3 million).
- Increasing the number of phases/tasks leads to a drop in performance for all training environments. Notably, the power-law does not collapse with the increase in the number of tasks; in fact, the gap between the power-law

Training Environment	Avg test accuracy for different training data sizes per phase				
	10000 samples	20000 samples	30000 samples	40000 samples	50000 samples
Upper baseline	0.909 (± 0.003)	0.919 (± 0.002)	0.928 (± 0.003)	0.933 (± 0.003)	0.934 (± 0.001)
Power-law	0.826 (± 0.008)	0.856 (± 0.005)	0.873 (± 0.007)	0.886 (± 0.004)	0.898 (± 0.003)
EWC	0.597 (± 0.01)	0.635 (± 0.012)	0.687 (± 0.015)	0.716 (± 0.025)	0.738 (± 0.027)
EWC (Online)	0.507 (± 0.006)	0.542 (± 0.022)	0.593 (± 0.014)	0.639 (± 0.017)	0.659 (± 0.026)
Lower baseline	0.351 (± 0.028)	0.392 (± 0.023)	0.418 (± 0.03)	0.44 (± 0.018)	0.456 (± 0.017)

Table 3: Variations in test accuracy as a function of the amount of new training data introduced in each phase. The bracketed values indicate one SD when running experiments with $N = 5$ seeds.

Training environment	Avg test accuracy	
	10 phases	20 phases
Upper baseline	0.936 (± 0.003)	0.874 (± 0.003)
Power-law	0.901 (± 0.004)	0.851 (± 0.004)
EWC	0.743 (± 0.024)	0.523 (± 0.016)
EWC (online)	0.670 (± 0.016)	0.444 (± 0.013)
Lower baseline	0.472 (± 0.007)	0.424 (± 0.012)

Table 4: Variations in test accuracy in the final phase as we increase the number of phases in the unrestricted memory scenario. The bracketed values indicate one SD when running experiments with $N = 5$ seeds.

and the upper baseline narrows (10 tasks, Δ test accuracy = 0.35, 20 tasks, Δ test accuracy = 0.23).

These simulation results show the same human-like ability to remember previous tasks while learning new ones when the distribution of previous tasks follows a power law.

Persistence of mitigation behavior in different situations

We investigate whether power-law training environments continue to mitigate CI over variation in the number of tasks (Table 4), as described above, and also in the amount of data rehearsed after each task (Table 3) and the model size (Table 5), as described next.

Varying the sample size of each task in our dataset Reducing the number of MNIST images before creating the permutations increases the complexity of the learning task, as the models have to perform similarly on the test data with a limited training size. We investigate different training sizes in intervals of 10000 samples (10000 - 60000 samples) in the unrestricted memory scenario. The goal of these experiments is to analyze whether models trained in power-law setup collapse with less training data, or whether their performance remains comparable to the upper baseline.

Table 3 shows the performance of the models with different training data sizes. The power-law model continues to perform close to the upper baseline, and their performance continues to be better than all of the other techniques. Additionally, the accuracy of models trained in the lower baseline environment and the EWC technique collapses for smaller training data sizes. This shows that models trained in power-law environments perform well even on more difficult learning scenarios (i.e., those with fewer training samples).

Varying the number of hidden layers in the model Increasing the number of hidden layers can affect the perfor-

mance of models trained in different environments. The correlation between model complexity (size) and accuracy is not always direct and positive; it also depends upon the difficulty of the tasks. Here, we investigate whether model complexity affects performance and whether different model complexities continue to display CI mitigation.

Table 5 shows the performance of the models with different numbers of hidden layers. Note that the performance of the rehearsal methods in the power-law environment is close to the upper baseline for all model complexities. Also note that while the regularization-based models perform better with 1 hidden layer, their performance collapses with increasing model complexity. On the other hand, even while seeing more training samples, the models trained in power-law and upper baseline environments do not suffer from such a collapse, showing better and more robust mitigation of CI.

Forward Facilitation in the power-law environment

For the permuted MNIST problem, the model learns a new task in each phase. More tasks increase learning difficulty because the model has limited representational capacity. Ideally, a strong model should show forward facilitation, that is, it should learn later tasks faster because of having learned similar tasks before. We evaluate forward facilitation in different training environments by exploring the test accuracy of the *newly introduced task* in different phases, in conjunction with the overall test accuracy on all tasks. We hypothesize that models that show better forward facilitation will see a relatively smaller drop in performance in the newly learned introduced tasks as the model weights reach their representational capacity, while at the same time maintaining performance on the previous tasks. We create a new metric termed the **forward facilitation score** that balances between the performance of the newly learned task and the performance of all tasks by their harmonic mean as given in equation (2).

$$FF - score = \frac{2 * Acc_{new-task} * Acc_{all-tasks}}{Acc_{new-task} + Acc_{all-tasks}} \quad (2)$$

Table 6 shows the *average test accuracy for the newly introduced task* after different phases of training. Note that while the lower baseline shows great performance on the test accuracy of the newly introduced task, it shows significant CI and forgets old tasks, as evidenced by its low forward facilitation score. For the other environments, through phase 10, we observe that the EWC model shows high accuracy on the newly introduced task in each respective phase, and also shows great forward facilitation. However, beyond phase 10, the EWC model collapses, showing poor forward facilitation. On the other, the power-law training environment shows

Training Environment	Avg test accuracy for different training data sizes per phase				
	1 Hidden Layer	2 Hidden Layers	3 Hidden Layers	4 Hidden Layers	5 Hidden Layers
Upper baseline	0.944 (± 0.003)	0.936 (± 0.002)	0.936 (± 0.002)	0.937 (± 0.002)	0.939 (± 0.001)
Power-law	0.929 (± 0.002)	0.882 (± 0.004)	0.901 (± 0.004)	0.913 (± 0.004)	0.915 (± 0.002)
EWC	0.897 (± 0.003)	0.88 (± 0.006)	0.747 (± 0.026)	0.657 (± 0.058)	0.603 (± 0.06)
EWC (online)	0.906 (± 0.003)	0.828 (± 0.007)	0.669 (± 0.022)	0.587 (± 0.033)	0.539 (± 0.054)
Lower baseline	0.608 (± 0.008)	0.477 (± 0.013)	0.472 (± 0.007)	0.512 (± 0.007)	0.534 (± 0.013)

Table 5: Variations in test accuracy in the final phase as we increase the model depth. The bracketed values indicate one SD when running experiments with $N = 5$ seeds.

Training Environment	Avg. test accuracy for new tasks in different phases of training								
	Phase 4	Phase 6	Phase 8	Phase 10	Phase 12	Phase 14	Phase 16	Phase 18	Phase 20
Upper baseline	0.959 (± 0.005)	0.928 (± 0.006)	0.914 (± 0.012)	0.903 (± 0.002)	0.882 (± 0.006)	0.863 (± 0.023)	0.847 (± 0.019)	0.835 (± 0.014)	0.812 (± 0.007)
Power-law	0.976 (± 0.001)	0.973 (± 0.001)	0.97 (± 0.001)	0.969 (± 0.002)	0.966 (± 0.002)	0.966 (± 0.001)	0.966 (± 0.002)	0.963 (± 0.001)	0.962 (± 0.003)
EWC	0.973 (± 0.001)	0.965 (± 0.001)	0.949 (± 0.004)	0.923 (± 0.003)	0.887 (± 0.006)	0.841 (± 0.005)	0.799 (± 0.009)	0.748 (± 0.006)	0.705 (± 0.004)
EWC (online)	0.972 (± 0.001)	0.965 (± 0.002)	0.949 (± 0.002)	0.919 (± 0.004)	0.886 (± 0.004)	0.839 (± 0.005)	0.789 (± 0.01)	0.742 (± 0.007)	0.697 (± 0.005)
Lower baseline	0.979 (± 0.0)	0.978 (± 0.001)	0.976 (± 0.001)	0.976 (± 0.001)	0.975 (± 0.001)	0.974 (± 0.001)	0.975 (± 0.001)	0.974 (± 0.001)	0.974 (± 0.001)
Avg. Forward facilitation score across phases of training									
Upper baseline	0.966 (± 0.003)	0.943 (± 0.003)	0.93 (± 0.007)	0.92 (± 0.002)	0.904 (± 0.003)	0.888 (± 0.014)	0.873 (± 0.01)	0.862 (± 0.009)	0.842 (± 0.004)
Power-law	0.972 (± 0.001)	0.963 (± 0.001)	0.952 (± 0.002)	0.945 (± 0.001)	0.935 (± 0.002)	0.927 (± 0.002)	0.92 (± 0.001)	0.911 (± 0.002)	0.903 (± 0.003)
EWC	0.919 (± 0.004)	0.89 (± 0.009)	0.864 (± 0.01)	0.825 (± 0.017)	0.784 (± 0.01)	0.729 (± 0.013)	0.679 (± 0.011)	0.643 (± 0.011)	0.6 (± 0.012)
EWC (online)	0.904 (± 0.006)	0.857 (± 0.008)	0.818 (± 0.019)	0.775 (± 0.015)	0.72 (± 0.014)	0.665 (± 0.013)	0.618 (± 0.017)	0.575 (± 0.014)	0.543 (± 0.01)
Lower baseline	0.772 (± 0.017)	0.702 (± 0.014)	0.653 (± 0.025)	0.632 (± 0.007)	0.623 (± 0.011)	0.615 (± 0.012)	0.613 (± 0.008)	0.603 (± 0.012)	0.59 (± 0.011)

Table 6: (a) Variations in the test accuracy for the newly introduced task across training phases in the unrestricted memory scenario. (b) Variations in the forward facilitation score across training phases. This score balances accuracy in learning a new task and remembering old tasks. The bracketed values indicate one SD when running experiments with $N = 5$ seeds.

Min. amount of samples of each previous task in a new phase	Accuracy
5%	0.925 (± 0.003)
2%	0.917 (± 0.003)
1%	0.901 (± 0.004)
0.1%	0.814 (± 0.01)
0.01%	0.706 (± 0.015)

Table 7: Variations in test accuracy as a function of the proportion of samples for each previous task in the last phase. The bracketed values indicate one SD when running experiments with $N = 5$ seeds.

virtually no drop in performance on the newly introduced task even during phase 20. *Performance of the new task in the power-law environment is almost as good as the performance of the lower baseline on the new task without the same forgetting of old tasks.* This indicates superior forward facilitation capabilities of the power-law environment over all other environments considered in this study.

How much old training data must be maintained in each phase to observe mitigation of CI?

In every phase after phase 2, task 1 has the smallest representation in the rehearsal data. By varying this, we test the minimum amount of rehearsal data required for an old task to maintain the mitigation of CI. Most experiments presented in this paper for the power-law environment assume that the minimum number of samples in the last phase for task 1 is 1% of the original training size of each task. In this section, we explore how varying this minimum data value affects the performance of models trained in a power-law setup.

Table 7 shows the performance of the power-law models after training on 10 tasks over 10 phases when varying the

minimum number of samples with five different sample percentages. Only when the minimum number drops below 1% of the task sample size is there a considerable decline in the performance of the model. At 0.1%, model accuracy begins to collapse. Thus, we use 1% as the minimum number of samples for the least represented task in the last phase in our experiments.

Restricted memory scenario

We simulate the reality of memory budgets and set fixed rehearsal data proportions for three training environments: uniform (ER), power-law, and exponential.

Table 8 shows the accuracy of models in these three training environments with 7 rehearsal sizes (i.e., proportions): [0.001, 0.05, 0.1, 0.25, 0.5, 0.75, 1.0]. These sizes determine the fraction of previous data that is included relative to the new task data.

Our findings show that the accuracy of the model is sensitive to the rehearsal proportion and falls off quickly when this is a lower value such as 0.1. Because we are fixing the total data size, the accuracy will only be determined by the distribution function. Across all the proportion values, the trend is clear: the best distribution function is uniform for maintaining high accuracy, and the worst is exponential. One reason for the lower performance of exponential distribution might be that this function falls off very quickly, which results in a much lower representation of previous tasks with each new phase. The positive results for the uniform distribution are somewhat expected: if the same amount of previous data is seen every time the model learns something new, then it can continue recalling the previous tasks because it gets a chance to reinforce the existing knowledge.

Although the power-law distribution declines, it does not

Training Environment	Avg test accuracy for different Rehearsal sizes						
	RS: 0.01	RS: 0.05	RS: 0.1	RS: 0.25	RS: 0.5	RS: 0.75	RS: 1.0
Uniform	0.531 (± 0.008)	0.808 (± 0.012)	0.838 ± 0.01	0.898 ± 0.006	0.925 ± 0.004	0.929 ± 0.001	0.932 (± 0.003)
Power-law	0.516 (± 0.012)	0.776 (± 0.013)	0.82 ± 0.008	0.88 ± 0.007	0.911 ± 0.003	0.922 ± 0.003	0.926 (± 0.002)
Exponential	0.484 (± 0.006)	0.675 (± 0.017)	0.72 ± 0.013	0.793 ± 0.009	0.843 ± 0.007	0.859 ± 0.006	0.865 (± 0.007)

Table 8: Variations in test accuracy in the final phase for different rehearsal proportions. The bracketed values indicate one SD when running experiments with $N = 5$ seeds. RS is Rehearsal Size.

do so as rapidly as the exponential distribution, and the results show clearly that performance in the power-law training environment performance is much closer to the uniform distribution than it is to the exponential distribution. Thus, the power-law resembles the best interleaving environment.

Despite the better results of uniform distribution, it might not always be possible for the learner to dictate the nature of the training environment. Thus it is reassuring that when the learner has no control over the training environment, to the degree that it resembles the naturalistic (i.e., power-law) environment of human learning, then similar levels of accuracy can be achieved. From Table 8, we can see that there is a sharp fall in model accuracy as the proportion falls below 0.5, where the lowest accuracy of the power-law distributed model decreases below 90% to 80% when the proportion is 0.1, and further collapses to near 50% when the proportion is 0.001, the smallest value tested in our experiments. This shows that along with distribution, the rehearsal proportion is also important for maintaining high accuracy in successive phases.

Conclusion

We apply the naturalistic learning environments that humans experience to the continual learning problem in neural networks. Our simulations offer an evaluation of sequential learning capabilities and are realistic in accounting for memory constraints and budgeting strategies.

We train models in different environments on a Domain-IL scenario: permuted MNIST handwritten digit recognition tasks. The networks are trained on multiple phases to understand the extent of CI in different training setups. In the unrestricted memory scenario, where we don't restrict the replay data size, we observed that the models trained in the power-law environment perform comparably to models trained over all the previous data (i.e., the upper baseline). Thus, these models behave like humans in not forgetting previous tasks when they continue to encounter new tasks in a decreasing power-law manner. We introduce a new metric to quantify forward facilitation - the harmonic mean of the averaged accuracy on old tasks and the accuracy of the new task. Under this new metric, we also observe that power-law has better forward facilitation (i.e., transfer of learning) than models trained in the upper baseline environments, and that when the number of phases is increased, the new task accuracy in the power-law model does not suffer compared to the EWC approach. In the unrestricted setup, we see that the models trained in the power-law training environment perform better than those trained in the exponential environment, and have comparable accuracy to those trained in the uniform environment. Overall, our experiments demonstrate that the

power-law training environment can mitigate CI; as such, it provides a new baseline for future research in continual learning.

Ethical considerations

There are no major risks associated with conducting this research beyond those associated with developing any machine learning training paradigms.

Limitations and Future Works

For all the experiments reported here, we had fixed dropout probability, learning rate, batch size, maximum training iterations per task, and number of units per layer. We do not carry out experiments with different loss functions and optimizers. Also, we do not implement early stopping. The results can be somewhat different if we use optimal parameters obtained from grid search; however, our current results show that the difference between the performance of power-law and other approaches is significant even when the sample size and the model complexity are varied. Our experiments do not compare the power-law model with other well-known replay-based approaches like LwF (Learning without Forgetting), DGR (Deep Generative Replay) (Shin et al. 2017b), and regularization-based approaches like Synaptic Intelligence (SI).

Also, our experiments test Domain-IL tasks that are artificially generated from the MNIST handwritten digit dataset. Future work can test the ideas presented in this work to a more challenging set of tasks (Class Incremental Learning) such as image recognition with colored input as in the CIFAR dataset (Krizhevsky, Hinton et al. 2009) or both color and texture-based images as found in the CLEVR dataset (Johnson et al. 2016). The models utilized to solve these problems would also be more complex CNN-based architectures and might provide more insight into the capabilities and drawbacks of utilizing a power-law training environment to mitigate CI.

References

- Abello; Buchsbaum; and Westbrook. 2002. A functional approach to external graph algorithms. *Algorithmica*, 32: 437–458.
- Aiello, W.; Chung, F.; and Lu, L. 2000. A random graph model for massive graphs. In *Proceedings of the thirty-second annual ACM symposium on Theory of computing*, 171–180.
- Anderson, J. R.; and Schooler, L. J. 1991. Reflections of the Environment in Memory. *Psychological Science*, 2(6): 396–408.

- Anderson, R. B.; Tweney, R. D.; Rivardo, M.; and Duncan, S. 1997. Need probability affects retention: A direct demonstration. *Memory and Cognition*, 25(6): 867–872.
- Baird, L.; Evans, N.; and Greenhill, S. J. 2022. Blowing in the wind: Using ‘North Wind and the Sun’ texts to sample phoneme inventories. *Journal of the International Phonetic Association*, 52(3): 453–494.
- Bhardwaj, K.; Martin, D.; Singh, R.; Deshpande, G.; So, M.; Neubeur, W.; Mosur, P.; and Starner, T. 2024. PopSignAI : Using Sign Language Recognition to Improve American Sign Language Learning in Novice Signers.
- Cvetojevic, S.; and Hochmair, H. H. 2018. Analyzing the spread of tweets in response to Paris attacks. *Computers, Environment and Urban Systems*, 71: 14–26.
- Dai, Y.; Lang, H.; Zheng, Y.; Yu, B.; Huang, F.; and Li, Y. 2023. Domain Incremental Lifelong Learning in an Open World. arXiv:2305.06555.
- Davidson, G.; and Mozer, M. C. 2020. Sequential mastery of multiple visual tasks: Networks naturally learn to learn and forget to forget. In *The IEEE Conference on Computer Vision and Pattern Recognition (CVPR)*.
- Deng, L. 2012. The MNIST Database of Handwritten Digit Images for Machine Learning Research [Best of the Web]. *IEEE Signal Processing Magazine*, 29(6): 141–142.
- Goodfellow, I. J.; Mirza, M.; Xiao, D.; Courville, A.; and Bengio, Y. 2015. An Empirical Investigation of Catastrophic Forgetting in Gradient-Based Neural Networks. arXiv:1312.6211.
- Hayes, T. L.; Kaffle, K.; Shrestha, R.; Acharya, M.; and Kanan, C. 2019. REMIND Your Neural Network to Prevent Catastrophic Forgetting. *CoRR*, abs/1910.02509.
- Hayes, T. L.; and Kanan, C. 2019. Lifelong Machine Learning with Deep Streaming Linear Discriminant Analysis. *CoRR*, abs/1909.01520.
- Holme, P.; Karlin, J.; and Forrest, S. 2007. Radial structure of the Internet. *Proceedings of the Royal Society A: Mathematical, Physical and Engineering Sciences*, 463(2081): 1231–1246.
- Ito, T.; Tashiro, K.; Muta, S.; Ozawa, R.; Chiba, T.; Nishizawa, M.; Yamamoto, K.; Kuhara, S.; and Sakaki, Y. 2000. Toward a protein–protein interaction map of the budding yeast: a comprehensive system to examine two-hybrid interactions in all possible combinations between the yeast proteins. *Proceedings of the National Academy of Sciences*, 97(3): 1143–1147.
- Johnson, J.; Hariharan, B.; van der Maaten, L.; Fei-Fei, L.; Zitnick, C. L.; and Girshick, R. 2016. CLEVR: A Diagnostic Dataset for Compositional Language and Elementary Visual Reasoning. arXiv:1612.06890.
- Kemker, R.; and Kanan, C. 2017. FearNet: Brain-Inspired Model for Incremental Learning. *CoRR*, abs/1711.10563.
- Kirkpatrick, J.; Pascanu, R.; Rabinowitz, N.; Veness, J.; Desjardins, G.; Rusu, A. A.; Milan, K.; Quan, J.; Ramalho, T.; Grabska-Barwinska, A.; et al. 2017. Overcoming catastrophic forgetting in neural networks. *Proceedings of the national academy of sciences*, 114(13): 3521–3526.
- Kirkpatrick, J.; Pascanu, R.; Rabinowitz, N. C.; Veness, J.; Desjardins, G.; Rusu, A. A.; Milan, K.; Quan, J.; Ramalho, T.; Grabska-Barwinska, A.; Hassabis, D.; Clopath, C.; Kumaran, D.; and Hadsell, R. 2016. Overcoming catastrophic forgetting in neural networks. *CoRR*, abs/1612.00796.
- Krizhevsky, A.; Hinton, G.; et al. 2009. Learning multiple layers of features from tiny images.
- Lee, S.-W.; Kim, J.-H.; Jun, J.; Ha, J.-W.; and Zhang, B.-T. 2017. Overcoming catastrophic forgetting by incremental moment matching. *Advances in neural information processing systems*, 30.
- Li, Z.; and Hoiem, D. 2017. Learning without forgetting. *IEEE transactions on pattern analysis and machine intelligence*, 40(12): 2935–2947.
- Lopez-Paz, D.; and Ranzato, M. 2017. Gradient Episodic Memory for Continuum Learning. *CoRR*, abs/1706.08840.
- Lu, Y.; Zhang, P.; Cao, Y.; Hu, Y.; and Guo, L. 2014. On the frequency distribution of retweets. *Procedia Computer Science*, 31: 747–753.
- Lyndgaard, S.; Tidler, Z. R.; Provine, L.; and Varma, S. 2022. Catastrophic interference in neural network models is mitigated when the training data reflect a power-law environmental structure. In *Proceedings of the Annual Meeting of the Cognitive Science Society*, volume 44.
- Mallya, A.; and Lazebnik, S. 2018. Packnet: Adding multiple tasks to a single network by iterative pruning. In *Proceedings of the IEEE conference on Computer Vision and Pattern Recognition*, 7765–7773.
- McCloskey, M.; and Cohen, N. J. 1989. Catastrophic Interference in Connectionist Networks: The Sequential Learning Problem. volume 24 of *Psychology of Learning and Motivation*, 109–165. Academic Press.
- Meir, Y.; Sardi, S.; Hodassman, S.; Kisos, K.; Ben-Noam, I.; Goldental, A.; and Kanter, I. 2020. Power-law scaling to assist with key challenges in artificial intelligence. *Scientific reports*, 10(1): 19628.
- Milojević, S. 2010. Power law distributions in information science: Making the case for logarithmic binning. *Journal of the American Society for Information Science and Technology*, 61(12): 2417–2425.
- Mitchell, T.; Cohen, W.; Hruschka, E.; Talukdar, P.; Yang, B.; Betteridge, J.; Carlson, A.; Dalvi, B.; Gardner, M.; Kisiel, B.; Krishnamurthy, J.; Lao, N.; Mazaitis, K.; Mohamed, T.; Nakashole, N.; Platanios, E.; Ritter, A.; Samadi, M.; Settles, B.; Wang, R.; Wijaya, D.; Gupta, A.; Chen, X.; Saparov, A.; Greaves, M.; and Welling, J. 2018. Never-Ending Learning. *Commun. ACM*, 61(5): 103–115.
- Nadini, M.; Alessandretti, L.; Di Giacinto, F.; Martino, M.; Aiello, L. M.; and Baronchelli, A. 2021. Mapping the NFT revolution: market trends, trade networks, and visual features. *Scientific reports*, 11(1): 20902.
- Newell, A.; and Rosenbloom, P. S. 2013. Mechanisms of skill acquisition and the law of practice. In *Cognitive skills and their acquisition*, 1–55. Psychology Press.
- Newman, M. E. 2005. Power laws, Pareto distributions and Zipf’s law. *Contemporary physics*, 46(5): 323–351.

Parisi, G. I.; Kemker, R.; Part, J. L.; Kanan, C.; and Wermter, S. 2019. Continual lifelong learning with neural networks: A review. *Neural Networks*, 113: 54–71.

Paszke, A.; Gross, S.; Massa, F.; Lerer, A.; Bradbury, J.; Chanan, G.; Killeen, T.; Lin, Z.; Gimelshein, N.; Antiga, L.; Desmaison, A.; Kopf, A.; Yang, E.; DeVito, Z.; Raison, M.; Tejani, A.; Chilamkurthy, S.; Steiner, B.; Fang, L.; Bai, J.; and Chintala, S. 2019. PyTorch: An Imperative Style, High-Performance Deep Learning Library. In Wallach, H.; Larochelle, H.; Beygelzimer, A.; d'Alché-Buc, F.; Fox, E.; and Garnett, R., eds., *Advances in Neural Information Processing Systems 32*, 8024–8035. Curran Associates, Inc.

Rebuffi, S.; Kolesnikov, A.; and Lampert, C. H. 2016. iCaRL: Incremental Classifier and Representation Learning. *CoRR*, abs/1611.07725.

Robins, A. 1995. Catastrophic forgetting, rehearsal and pseudorehearsal. *Connection Science*, 7(2): 123–146.

Rolnick, D.; Ahuja, A.; Schwarz, J.; Lillicrap, T. P.; and Wayne, G. 2018. Experience Replay for Continual Learning. *CoRR*, abs/1811.11682.

Rusu, A. A.; Rabinowitz, N. C.; Desjardins, G.; Soyer, H.; Kirkpatrick, J.; Kavukcuoglu, K.; Pascanu, R.; and Hadsell, R. 2022. Progressive Neural Networks. arXiv:1606.04671.

Schooler, L. J.; and Anderson, J. R. 1997. The Role of Process in the Rational Analysis of Memory. *Cognitive Psychology*, 32(3): 219–250.

Schwarz, J.; Luketina, J.; Czarnecki, W. M.; Grabska-Barwinska, A.; Teh, Y. W.; Pascanu, R.; and Hadsell, R. 2018. Progress & Compress: A scalable framework for continual learning. arXiv:1805.06370.

Serra, J.; Suris, D.; Miron, M.; and Karatzoglou, A. 2018. Overcoming catastrophic forgetting with hard attention to the task. In *International conference on machine learning*, 4548–4557. PMLR.

Shin, H.; Lee, J. K.; Kim, J.; and Kim, J. 2017a. Continual Learning with Deep Generative Replay. *CoRR*, abs/1705.08690.

Shin, H.; Lee, J. K.; Kim, J.; and Kim, J. 2017b. Continual Learning with Deep Generative Replay. arXiv:1705.08690.

Stevens, J. R.; Marewski, J. N.; Schooler, L. J.; and Gilby, I. C. 2016. Reflections of the social environment in chimpanzee memory: applying rational analysis beyond humans. *Royal Society Open Science*, 3(8): 160293.

Thrun, S.; and O’Sullivan, J. 1996. Discovering Structure in Multiple Learning Tasks: The TC Algorithm. In *Proceedings of the Thirteenth International Conference on International Conference on Machine Learning*, ICML’96, 489–497. San Francisco, CA, USA: Morgan Kaufmann Publishers Inc. ISBN 1558604197.

van de Ven, G. M.; Siegelmann, H. T.; and Tolias, A. S. 2020. Brain-inspired replay for continual learning with artificial neural networks. *Nature Communications*, 11(1): 4069.

van de Ven, G. M.; and Tolias, A. S. 2019. Three scenarios for continual learning. arXiv:1904.07734.

van de Ven, G. M.; Tuytelaars, T.; and Tolias, A. S. 2022. Three types of incremental learning. *Nature Machine Intelligence*, 4(12): 1185–1197.

Wang, L.; Zhang, X.; Su, H.; and Zhu, J. 2023. A Comprehensive Survey of Continual Learning: Theory, Method and Application. arXiv:2302.00487.

Xie, Y.; Pan, Z.; Ma, J.; Jie, L.; and Mei, Q. 2023. A Prompt Log Analysis of Text-to-Image Generation Systems. In *Proceedings of the ACM Web Conference 2023*, WWW ’23. ACM.

Xu, Y.; Furao, S.; Hasegawa, O.; and Zhao, J. 2009. An Online Incremental Learning Vector Quantization. In Theeramunkong, T.; Kijssirikul, B.; Cercone, N.; and Ho, T.-B., eds., *Advances in Knowledge Discovery and Data Mining*, 1046–1053. Berlin, Heidelberg: Springer Berlin Heidelberg. ISBN 978-3-642-01307-2.

Zenke, F.; Poole, B.; and Ganguli, S. 2017. Continual learning through synaptic intelligence. In *International conference on machine learning*, 3987–3995. PMLR.

Appendix

Operationalization of restricted training environment
The operationalization of the restricted training environment can be configured to the problem type and complexity.

Modified power-law distribution: The following expression is used to generate values:

$$f(x) = \alpha \cdot x^{\alpha-1} \quad (3)$$

Here, α is a hyperparameter to be specified for generating the values. For the MNIST problem with 10 tasks, in the last phase, we need to generate nine values for the previous nine tasks learned in the initial phases. We sample values from distribution starting from 0.10 and every adjacent point is 0.01 units apart. Thus, for generating nine values, we sample the values at [0.10, 0.11, ..., 0.18]. Note that the generated values might not add up to the required sum value. In order to satisfy the constraint, each term is rescaled by the ratio of the required sum to the current sum of generated values. Proportional scaling ensures that the numbers still follow the power-law distribution while adding up to the desired value.

Modified exponential distribution: Similar to the power-law equation, the equation for the exponential distribution is as follows:

$$f(x) = \frac{1}{\beta} \cdot e^{-\frac{x}{\beta}} \quad (4)$$

In this training environment, β is a hyperparameter to be specified for generating the values.

In the last phase of permuted MNIST tasks, we need to generate nine values for the previous tasks learned in the prior phases. Similar to the power-law environment, we sample values from the exponential distribution, but here the sample points start from 1 and every adjacent sample point is 1 unit apart. Thus, for generating nine values, we sample the values ranging from 1 to 9. Note: Because the values might not add up to the required rehearsal value, we perform proportional rescaling. Proportional scaling ensures that the numbers still

Min. amount of samples of each previous task in a new phase (percentage of the total task size)	Constants		Power-law Equation
	a	b	
5%	60000	1.301	$60000 \cdot x^{-1.301}$
2%	60000	1.699	$60000 \cdot x^{-1.699}$
1%	60000	2	$60000 \cdot x^{-2}$
0.1%	60000	3	$60000 \cdot x^{-3}$
0.01%	60000	4	$60000 \cdot x^{-4}$

Table 9: Power-law constants and equation for different minimum number of samples for each previous task at the last phase

follow the exponential law distribution while adding up to the desired value.

Uniform distribution: The uniform distribution is the most trivial among all the rehearsal environments: each rehearsal data set contains an equal number of examples from all the previous tasks. Hence, the size of the rehearsal data is divided by the number of previous tasks and that provides the frequency for examples to pick from each of the previous tasks. This is analogous to the upper baseline but with rehearsal ratios.

Power-law distribution equation

The power-law sample distribution equation is given by equation (1), where the values for x range from one to the maximum number of phases. However, the constants a and b have to be calculated for getting the distribution equation for the power-law environment. These constants are calculated in the following manner:

$$a = \text{maxSamples}$$

$$b = -\frac{\log\left(\frac{\text{minSamples}}{\text{maxSamples}}\right)}{\log(\text{number of phases})}$$

where maxSamples = maximum number of samples when introducing a new task and minSamples = minimum number of samples of the first task in the last phase.

Table 9 shows the equation and the constant values for varying minimum numbers of samples for each previous task at the last phase.

Data distribution across phases in different environments

Part I: Distribution in unrestricted memory scenario Tables 10 show the distribution of training samples for each task in different phases of Lower Baseline, EWC, and EWC (online) training environments. Similarly, tables 11 and 12 show the distribution for training samples in upper baseline and power-law environments.

Part II: Distribution of training samples in restricted memory scenario The tables in this section show the distribution of training samples in different phases of 3 restricted environments in our paper: uniform, power-law, and exponential.

Uniform: Tables 13, 14, 15, shows data distribution in Uniform environment with rehearsal sizes: [0.1, 0.5, 1.0].

Power-law: Tables 16, 17, 18, shows data distribution in Uniform environment with rehearsal sizes: [0.1, 0.5, 1.0].

Exponential: Tables 19, 20, 21, shows data distribution in Uniform environment with rehearsal sizes: [0.1, 0.5, 1.0].

	Task 1	Task 2	Task 3	Task 4	Task 5	Task 6	Task 7	Task 8	Task 9	Task 10
Phase 1	60000	0	0	0	0	0	0	0	0	0
Phase 2	0	60000	0	0	0	0	0	0	0	0
Phase 3	0	0	60000	0	0	0	0	0	0	0
Phase 4	0	0	0	60000	0	0	0	0	0	0
Phase 5	0	0	0	0	60000	0	0	0	0	0
Phase 6	0	0	0	0	0	60000	0	0	0	0
Phase 7	0	0	0	0	0	0	60000	0	0	0
Phase 8	0	0	0	0	0	0	0	60000	0	0
Phase 9	0	0	0	0	0	0	0	0	60000	0
Phase 10	0	0	0	0	0	0	0	0	0	60000

Table 10: Data distribution for tasks in each phase in lower baseline, EWC and EWC (online) training environments

	Task 1	Task 2	Task 3	Task 4	Task 5	Task 6	Task 7	Task 8	Task 9	Task 10
Phase 1	60000	0	0	0	0	0	0	0	0	0
Phase 2	60000	60000	0	0	0	0	0	0	0	0
Phase 3	60000	60000	60000	0	0	0	0	0	0	0
Phase 4	60000	60000	60000	60000	0	0	0	0	0	0
Phase 5	60000	60000	60000	60000	60000	0	0	0	0	0
Phase 6	60000	60000	60000	60000	60000	60000	0	0	0	0
Phase 7	60000	60000	60000	60000	60000	60000	60000	0	0	0
Phase 8	60000	60000	60000	60000	60000	60000	60000	60000	0	0
Phase 9	60000	60000	60000	60000	60000	60000	60000	60000	60000	0
Phase 10	60000	60000	60000	60000	60000	60000	60000	60000	60000	60000

Table 11: Data distribution for tasks in each phase in upper baseline training environment

	Task 1	Task 2	Task 3	Task 4	Task 5	Task 6	Task 7	Task 8	Task 9	Task 10
Phase 1	60000	0	0	0	0	0	0	0	0	0
Phase 2	15000	60000	0	0	0	0	0	0	0	0
Phase 3	6666	15000	60000	0	0	0	0	0	0	0
Phase 4	3750	6666	15000	60000	0	0	0	0	0	0
Phase 5	2400	3750	6666	15000	60000	0	0	0	0	0
Phase 6	1666	2400	3750	6666	15000	60000	0	0	0	0
Phase 7	1224	1666	2400	3750	6666	15000	60000	0	0	0
Phase 8	937	1224	1666	2400	3750	6666	15000	60000	0	0
Phase 9	740	937	1224	1666	2400	3750	6666	15000	60000	0
Phase 10	600	740	937	1224	1666	2400	3750	6666	15000	60000

Table 12: Data distribution for tasks in each phase in power-law unrestricted training environment

	Task 1	Task 2	Task 3	Task 4	Task 5	Task 6	Task 7	Task 8	Task 9	Task 10
Phase 1	60000	0	0	0	0	0	0	0	0	0
Phase 2	6000	60000	0	0	0	0	0	0	0	0
Phase 3	3000	3000	60000	0	0	0	0	0	0	0
Phase 4	2000	2000	2000	60000	0	0	0	0	0	0
Phase 5	1500	1500	1500	1500	60000	0	0	0	0	0
Phase 6	1200	1200	1200	1200	1200	60000	0	0	0	0
Phase 7	1000	1000	1000	1000	1000	1000	60000	0	0	0
Phase 8	857	857	857	857	857	857	857	60000	0	0
Phase 9	750	750	750	750	750	750	750	750	60000	0
Phase 10	666	666	666	666	666	666	666	666	666	60000

Table 13: Data distribution for tasks in each phase in a uniform training environment with rehearsal size 0.1

	Task 1	Task 2	Task 3	Task 4	Task 5	Task 6	Task 7	Task 8	Task 9	Task 10
Phase 1	60000	0	0	0	0	0	0	0	0	0
Phase 2	30000	60000	0	0	0	0	0	0	0	0
Phase 3	15000	15000	60000	0	0	0	0	0	0	0
Phase 4	10000	10000	10000	60000	0	0	0	0	0	0
Phase 5	7500	7500	7500	7500	60000	0	0	0	0	0
Phase 6	6000	6000	6000	6000	6000	60000	0	0	0	0
Phase 7	5000	5000	5000	5000	5000	5000	60000	0	0	0
Phase 8	4285	4285	4285	4285	4285	4285	4285	60000	0	0
Phase 9	3750	3750	3750	3750	3750	3750	3750	3750	60000	0
Phase 10	3333	3333	3333	3333	3333	3333	3333	3333	3333	60000

Table 14: Data Distribution for tasks in each phase in a uniform training environment with rehearsal size 0.5

	Task 1	Task 2	Task 3	Task 4	Task 5	Task 6	Task 7	Task 8	Task 9	Task 10
Phase 1	60000	0	0	0	0	0	0	0	0	0
Phase 2	60000	60000	0	0	0	0	0	0	0	0
Phase 3	30000	30000	60000	0	0	0	0	0	0	0
Phase 4	20000	20000	20000	60000	0	0	0	0	0	0
Phase 5	15000	15000	15000	15000	60000	0	0	0	0	0
Phase 6	12000	12000	12000	12000	12000	60000	0	0	0	0
Phase 7	10000	10000	10000	10000	10000	10000	60000	0	0	0
Phase 8	8571	8571	8571	8571	8571	8571	8571	60000	0	0
Phase 9	7500	7500	7500	7500	7500	7500	7500	7500	60000	0
Phase 10	6666	6666	6666	6666	6666	6666	6666	6666	6666	60000

Table 15: Data distribution for tasks in each phase in a uniform training environment with rehearsal size 1.0

	Task 1	Task 2	Task 3	Task 4	Task 5	Task 6	Task 7	Task 8	Task 9	Task 10
Phase 1	60000	0	0	0	0	0	0	0	0	0
Phase 2	5999	60000	0	0	0	0	0	0	0	0
Phase 3	2434	3565	60000	0	0	0	0	0	0	0
Phase 4	1322	1935	2741	60000	0	0	0	0	0	0
Phase 5	811	1188	1682	2317	60000	0	0	0	0	0
Phase 6	534	781	1107	1525	2051	60000	0	0	0	0
Phase 7	368	539	763	1051	1414	1863	60000	0	0	0
Phase 8	262	384	544	749	1008	1329	1720	60000	0	0
Phase 9	192	281	398	549	738	973	1260	1605	60000	0
Phase 10	143	210	298	410	552	728	942	1201	1510	60000

Table 16: Data distribution for tasks in each phase in a power-law training environment with rehearsal size 0.1

	Task 1	Task 2	Task 3	Task 4	Task 5	Task 6	Task 7	Task 8	Task 9	Task 10
Phase 1	60000	0	0	0	0	0	0	0	0	0
Phase 2	29999	60000	0	0	0	0	0	0	0	0
Phase 3	12174	17825	60000	0	0	0	0	0	0	0
Phase 4	6611	9679	13709	60000	0	0	0	0	0	0
Phase 5	4057	5940	8413	11588	60000	0	0	0	0	0
Phase 6	2670	3909	5536	7626	10257	60000	0	0	0	0
Phase 7	1840	2695	3816	5257	7071	9318	60000	0	0	0
Phase 8	1312	1922	2722	3749	5043	6646	8603	60000	0	0
Phase 9	961	1407	1993	2745	3693	4867	6300	8029	60000	0
Phase 10	719	1053	1491	2054	2763	3641	4714	6008	7552	60000

Table 17: Data distribution for tasks in each phase in a power-law training environment with rehearsal size 0.5

	Task 1	Task 2	Task 3	Task 4	Task 5	Task 6	Task 7	Task 8	Task 9	Task 10
Phase 1	60000	0	0	0	0	0	0	0	0	0
Phase 2	59999	60000	0	0	0	0	0	0	0	0
Phase 3	24349	35650	60000	0	0	0	0	0	0	0
Phase 4	13222	19359	27418	60000	0	0	0	0	0	0
Phase 5	8114	11881	16827	23176	60000	0	0	0	0	0
Phase 6	5340	7818	11073	15252	20515	60000	0	0	0	0
Phase 7	3681	5390	7633	10514	14142	18637	60000	0	0	0
Phase 8	2625	3844	5444	7499	10086	13292	17207	60000	0	0
Phase 9	1922	2815	3987	5491	7386	9734	12601	16059	60000	0
Phase 10	1438	2106	2983	4109	5527	7283	9429	12017	15104	60000

Table 18: Data distribution for tasks in each phase in a power-law training environment with rehearsal size 1.0

	Task 1	Task 2	Task 3	Task 4	Task 5	Task 6	Task 7	Task 8	Task 9	Task 10
Phase 1	60000	0	0	0	0	0	0	0	0	0
Phase 2	5999	60000	0	0	0	0	0	0	0	0
Phase 3	1613	4386	60000	0	0	0	0	0	0	0
Phase 4	540	1468	3991	60000	0	0	0	0	0	0
Phase 5	192	522	1421	3863	60000	0	0	0	0	0
Phase 6	69	190	516	1404	3818	60000	0	0	0	0
Phase 7	25	69	189	514	1398	3802	60000	0	0	0
Phase 8	9	25	69	188	513	1396	3796	60000	0	0
Phase 9	3	9	25	69	188	513	1395	3793	60000	0
Phase 10	1	3	9	25	69	188	513	1395	3792	60000

Table 19: Data distribution for tasks in each phase in an exponential training environment with rehearsal size 0.1

	Task 1	Task 2	Task 3	Task 4	Task 5	Task 6	Task 7	Task 8	Task 9	Task 10
Phase 1	60000	0	0	0	0	0	0	0	0	0
Phase 2	29999	60000	0	0	0	0	0	0	0	0
Phase 3	8068	21931	60000	0	0	0	0	0	0	0
Phase 4	2700	7341	19957	60000	0	0	0	0	0	0
Phase 5	961	2614	7106	19317	60000	0	0	0	0	0
Phase 6	349	950	2583	7023	19092	60000	0	0	0	0
Phase 7	128	348	946	2572	6993	19010	60000	0	0	0
Phase 8	47	127	347	944	2568	6982	18980	60000	0	0
Phase 9	17	47	127	347	944	2567	6978	18969	60000	0
Phase 10	6	17	47	127	347	944	2566	6977	18965	60000

Table 20: Data distribution for tasks in each phase in an exponential training environment with rehearsal size 0.5

	Task 1	Task 2	Task 3	Task 4	Task 5	Task 6	Task 7	Task 8	Task 9	Task 10
Phase 1	60000	0	0	0	0	0	0	0	0	0
Phase 2	59999	60000	0	0	0	0	0	0	0	0
Phase 3	16136	43863	60000	0	0	0	0	0	0	0
Phase 4	5401	14683	39914	60000	0	0	0	0	0	0
Phase 5	1923	5228	14212	38634	60000	0	0	0	0	0
Phase 6	699	1901	5167	14047	38184	60000	0	0	0	0
Phase 7	256	696	1892	5145	13987	38021	60000	0	0	0
Phase 8	94	255	695	1890	5137	13965	37961	60000	0	0
Phase 9	34	94	255	694	1888	5134	13957	37939	60000	0
Phase 10	12	34	94	255	694	1888	5133	13954	37931	60000

Table 21: Data distribution for tasks in each phase in an exponential training environment with rehearsal size 1.0